

Neural Network for Quantum Brain Dynamics: 4D $CP^1+U(1)$ Gauge Theory on Lattice and its Phase Structure

Shinya Sakane, Takashi Hiramatsu, and Tetsuo Matsui

Department of Physics, Kindai University
Higashi-Osaka, Japan 577-8502

Abstract. We consider a system of two-level quantum quasi-spins and gauge bosons put on a 3+1D lattice. As a model of neural network of the brain functions, these spins describe neurons quantum-mechanically, and the gauge bosons describes weights of synaptic connections. It is a generalization of the Hopfield model to a quantum network with dynamical synaptic weights. At the microscopic level, this system becomes a model of quantum brain dynamics proposed by Umezawa et al., where spins and gauge field describe water molecules and photons, respectively. We calculate the phase diagram of this system under quantum and thermal fluctuations, and find that there are three phases; confinement, Coulomb, and Higgs phases. Each phase is classified according to the ability to learn patterns and recall them. By comparing the phase diagram with that of classical networks, we discuss the effect of quantum fluctuations and thermal fluctuations (noises in signal propagations) on the brain functions.

Keywords: Hopfield Model, Gauge Neural Network, Quantum Brain Dynamics

1 Introduction

Various functions of the human brain such as awareness, learning, and recalling patterns have been subjects of intense studies in wide area of science including neuroscience, medical science, psychology. A widely adopted approach in these studies is to model the brain by a neural network (network of neurons) and simulate its static and dynamical properties. A well known example of such network is the Hopfield model [1], which offers us an interesting mechanism of associative memory (recalling memorized patterns of neurons).

In the Hopfield model, each neuron may have two states (fired or not) and the state of the i -th neuron is described by the Ising ($Z(2)$) variable $S_i (= \pm 1)$ ($i = 1, \dots, N$). S_i represents the scaled membrane potential as $S_i = 1$ (fired) and $S_i = -1$ (not fired). The information of memorized patterns of S_i is stored here in the parameters J_{ij} , which are called synaptic weights, through the Hebb's rule [2]. The time development of $S_i(t)$ ($t = 0, 1, 2, \dots$ is a discrete time) is intrinsically

deterministic, but, due to noises in signal propagation, it becomes random. This situation is modeled by introducing the energy $E(S_i(t), J_{ij})$ and considering statistical mechanics with Boltzmann distribution $P(S_i) \propto \exp[-\beta E(S_i, J_{ij})]$ where the effective “temperature” $T \equiv 1/\beta$ starts from zero (no noise) and rises as noise increases. Then the system is regarded as an Ising spin system with random (long-range) interactions J_{ij} . The phase diagram is calculable and consists of three phases; spin-ordered phase, spin-disordered phase, spin-glass phase according to the values of J_{ij} and β . The spin-ordered (ferromagnetic) phase corresponds to the state of successful recalling of learned patterns of S_i , while the spin-disorders (paramagnetic) phase to failed recalling, and the spin-glass phase to failed learning due to more patterns than the capacity.

As the next step, by regarding synaptic weights connecting neurons as plastic dynamical variables, various models of learning patterns have been proposed [3]. In Refs. [4,5] a set of new networks for learning have been proposed by promoting synaptic-weight parameters J_{ij} appeared in the Hopfield model to a dynamical gauge field $J_{ij}(t)$ (t is the time). The energy of these gauge neural networks respects gauge symmetry. Introduction of gauge theory as a model of brain functions is motivated from the function of synaptic weight itself. Let us consider the electric signal which starts from the neuron j and arrives at the neuron i . The electric potential transported by this signal is modulated from the initial value S_j at j to $J_{ij}S_j$ at i through the synapse. The synaptic weight J_{ij} is just the conversion factor of propagating potential. That is, J_{ij} expresses relative difference of two frames of potential at j and i . Any quantity having this nature, i.e., a measure of relative orientations of local frames, is to be called a gauge field. The gauge symmetry just implies that observable quantities such as energy should be independent of change of local frames as it should be. By treating these gauge models as models in statistical mechanics, we calculated their phase diagrams. Generally, they consist of three phases; confinement phase, Coulomb phase and Higgs phase. Each phase is characterized by the ability of learning patterns and recalling them (See Table I).

Our common sense tells us that the brain functions have nothing to do with quantum theory (or quantum effect is negligibly small). However, as long as our brain is made of atoms and molecules at the microscopic level, the microscopic model of the brain itself should be described in terms of these atoms and molecules. If we are involved in the enterprise of describing and understanding

Table I: Three phases of gauge neural network and abilities of learning and recalling patterns of S_i [4,5]. $\langle O \rangle$ is the Boltzmann average of O . $\langle J_{ij} \rangle \neq 0$ implies that J_{ij} has small fluctuations around the average (given by Hebb’s law [2]), and the enough information of memorized patterns are stored in J_{ij} , while $\langle J_{ij} \rangle = 0$ implies that strong fluctuations wash out such information. Similarly $\langle S_i \rangle \neq 0$ implies that S_i sustains an almost definite pattern, while $\langle S_i \rangle = 0$ implies S_i is totally unfocused.

Phase	$\langle J_{ij} \rangle$	$\langle S_i \rangle$	ability of learning	ability of recalling
Higgs	$\neq 0$	$\neq 0$	yes	yes
Coulomb	$\neq 0$	0	yes	no
Confinement	0	0	no	no

the brain functions by a framework of physics, our task should be relating such microscopic quantum model to widely studied neural networks at the macroscopic level and calculating the quantum effect upon them quantitatively. This paper concerns these two points.

In Sec. 2 we briefly explain quantum field theory proposed by Umezawa et al. [6] as a model of brain dynamics at the microscopic level. It consists of two-level quasi-spin variables describing dielectric dipoles of water molecules and bosons describing photons inside the brain which mediate the electromagnetic (EM) forces between dipoles. We respect the U(1) gauge invariance of EM interaction and introduce the $CP^1+U(1)$ lattice gauge theory put on a 4D lattice (3 spatial directions and 1 imaginary-time direction for path-integral quantization) as its lattice version. Introduction of a lattice model is to discuss an effective model at semi-macroscopic scales through renormalization. We then discuss that this lattice gauge theory itself may be regarded also as an effective GNN after parameters of the model are renormalized through coarse graining.

In Sec.3 we calculate the phase diagram of this 4D $CP^1+U(1)$ lattice gauge theory for general parameters and characterize each phase of Table I by measuring electric field, magnetic field, and magnetic monopole density. By considering this model as a GNN, we discuss the ability of learning and recalling patterns in each phase, and the quantum and thermal(noise) effects upon that ability by referring to the results of classical GNN's.

2 Quantum Brain Dynamics and the 4D $CP^1 + U(1)$ Lattice Gauge Theory

Umezawa et al. [6] proposed a quantum spin-boson model that may describe the brain at the microscopic level, and argued that memories may be stored in the ordered ground state and low-energy excitations. They considered a system of N atoms which interact through exchanging bosons. The m -th atom ($m = 1, \dots, N$) is described by $s = 1/2$ SU(2) pseudo-spin operators $\mathbf{S}_m = (S_{m1}, S_{m2}, S_{m3})$, and a boson having a 3D momentum k and energy $E(k)$ is described by canonical annihilation operator C_k and creation operator C_k^\dagger . Its Hamiltonian H is given by

$$H = \sum_k E_k C_k^\dagger C_k + \epsilon \sum_m S_{m3} - f \sum_m (C_m S_{m+} + \text{H.c.}), \quad (1)$$

where $S_{m+} = S_{m1} + iS_{m2}$ is the spin rising operator and C_m is the Fourier transform of C_k . Each term expresses energy of bosons, level splitting of spins by external field, and emission and absorption of bosons and associated spin flips. Jibu and Yasue [7] argued that the quasi-spins and bosons in Eq. (1) have explicit counterparts in the human brain; each quasi-spin \mathbf{S}_m describes an electric dipole moment of each molecule of bound water (water molecules stand almost still) and the bosons C_k describe evanescent photons mediating short-range interaction among dipoles.

To pursue this interpretation further and improve a couple of points of the model (1), we introduce a model with the following properties; (i) manifest U(1) local gauge invariance of EM interaction; (ii) self-consistently determined photon energy $E(k)$ (massive or massless); (iii) a lattice model with a cut-off scale to make renormalization-group transformation straightforward. It is a $\text{CP}^1 + \text{U}(1)$ lattice gauge theory defined on the 4D hyper-cubic lattice, a variation of Wilson's lattice gauge theory[8] by replacing fermionic quark variables by the CP^1 spin variables. We shall work in the path-integral representation of the partition function, $Z = \text{Tr} \exp(-\beta H)$. The imaginary time $\tau (\in [0, \beta])$ is also discretized with the lattice spacing a_0 . We use $x = (x_0, x_1, x_2, x_3)$ as the site index of the 4D hypercubic lattice, and $x_1, x_2, x_3 = 0, 1, \dots, N-1$ and $x_0 = 0, 1, \dots, N_0-1$ and $\beta = N_0 \times a_0$. We use $\mu = 0, 1, 2, 3$ as the direction index and also as the unit vector in the μ -th direction. The lattice spacing $a_\mu = (a_0, a, a, a)$ is regarded as a parameter to set the scale of the model in the sense of renormalization group. The $s = 1/2$ spins are described by the so-called CP^1 (complex projective) variables $z_{x\sigma} (\sigma = 1, 2)$ on each site x , a two-component complex variables satisfying $|z_{x1}|^2 + |z_{x2}|^2 = 1$. On each link $(x, x + \mu)$ (straight path between two nearest-neighbor (NN) sites), we have a U(1) gauge variable, $U_{x\mu} = \exp(i\theta_{x\mu})$ [$\theta_{x\mu} \in (-\pi, +\pi)$]. In the naive continuum limit ($a_\mu \rightarrow 0$), it is expressed as $U_{x\mu} = \exp(igaA_\mu(x))$ where $A_\mu(x)$ is the vector potential and g is the gauge coupling constant[8]. $U_{x\mu}$ measures the relative orientation of the two internal coordinates which measure the wave function of charged particles at x and $x + \mu$ [8]. Then Z is written as

$$Z = \int [dU][dz] \exp(A[U, z]),$$

$$[dU] \equiv \prod_{x,\mu} dU_{x\mu} = \prod_{x,\mu} \frac{d\theta_{x\mu}}{2\pi}, \quad [dz] \equiv \prod_x dz_{x1} dz_{x2} \delta(|z_{x1}|^2 + |z_{x2}|^2 - 1). \quad (2)$$

$A[U, z]$ is the action of the model given by

$$A = \frac{c_1}{2} \sum_{x,\mu,\sigma} \left(\bar{z}_{x+\mu,\sigma} U_{x\mu} z_{x\sigma} + \text{c.c.} \right) + \frac{c_2}{2} \sum_{x,\mu < \nu} \left(\bar{U}_{x\nu} \bar{U}_{x+\nu,\mu} U_{x+\mu,\nu} U_{x\mu} + \text{c.c.} \right), \quad (3)$$

where c_1 and c_2 are real parameters of the model. These parameters are regarded to characterize each brain, i.e., each person has his(her) own values of c_1 and c_2 (and the other parameters for (irrelevant) interactions not included here). The action A is invariant under the following U(1) local (x -dependent) gauge transformation;

$$z_{xa} \rightarrow z'_{xa} = e^{i\Lambda_x} z_{xa}, \quad U_{x\mu} \rightarrow U'_{x\mu} = e^{i\Lambda_{x+\mu}} U_{x\mu} e^{-i\Lambda_x}. \quad (4)$$

Here we note that the partition function Z of (2) is a function of βc_1 and βc_2 . Below we set $\beta = 1$ in the most of expressions for simplicity. The β -dependence is easily recovered by replacing $c_{1(2)} \rightarrow \beta c_{1(2)}$. In the continuum limit $a, a_0 \rightarrow 0$, the c_1 -term of (3) becomes the kinetic term of z_x , while the c_2 -term becomes the electromagnetic action $\propto \mathbf{E}\mathbf{E} + \mathbf{B}\mathbf{B}$.

By applying the renormalization-group transformation to the model (2), one may obtain an effective theory at the lattice spacings $a'_\mu = \lambda a_\mu$. The analysis made for the related models of lattice gauge theory [9] shows that the relevant interactions at larger distances are the c_1 and c_2 terms and next-NN terms such as $\bar{z}UUUz$, $\bar{z}UUUUz$, and no qualitatively different terms emerge. Thus we think that the model (2) may be worth to study as an approximation of the effective model of neural network for the brain. In this viewpoint, the meaning of variables are as follows; (i) the CP^1 variable $z_{x\sigma}$ is the probability amplitude of quantum neuron state $|S_x\rangle = z_{x1}|1\rangle_x + z_{x2}|2\rangle_x$ where $|1\rangle$ and $|2\rangle$ are two independent states, such as fired or unfired, and (ii) the $\text{U}(1)$ variable $U_{x\mu} = \exp(i\theta_{x\mu})$ is the phase part of wave function of the synaptic connection weight between NN pair $(x, x + \mu)$. Therefore, by replacing $z_{x\sigma}$ and $U_{x\mu}$ by the neuron variable S_x and the synaptic weight variable $J_{x\mu}$ respectively, the action A of Eq. (3) is viewed as the action of GNN at macroscopic level;

$$A = \frac{c_1}{2} \sum \bar{S}_{x+\mu} J_{x+\mu, x} S_x + \frac{c_2}{2} \sum J_{x, x+\nu} J_{x+\nu, x+\mu+\nu} J_{x+\mu+\nu, x+\mu} J_{x+\mu, x} + \text{c.c.} \quad (5)$$

We note that its first term $c_1 SJS$ corresponds to the Hopfield energy [1] and the second term $c_2 JJJJ$ describes the reverberating current of signals explained in Ref. [2], which runs along a closed loop $(x \rightarrow x + \mu \rightarrow x + \mu + \nu \rightarrow x + \nu \rightarrow x)$.

Of course we recognize that the brain itself is far more complicated than this effective model; e.g., the network is multilayer with column structure and the synaptic connections are long-range and asymmetric (J_{ij} and J_{ji} are independent) with various strengths ($J_{ij} \in \mathbf{R}$). However, these points can be incorporated systematically into the present model (2) in the framework of quantum gauge theory as inputs in the stage of model building, and we leave them as future problems.

3 Phase Structure of the 4D $\text{CP}^1 + \text{U}(1)$ Gauge Theory

In this section we study the phase structure of the model (2) by Monte Carlo simulation (MCS) and discuss the effect of quantum and thermal fluctuations upon the ability of learning and recalling patterns.

3.1 Phase Diagram

In our MCS, we consider a hypercubic lattice of size L^4 with periodic boundary condition. This implies the corresponding ‘‘temperature’’ T tends to zero $T \rightarrow 0$ as the thermodynamic limit $L \rightarrow \infty$ is taken [9]. We use standard Metropolis algorithm to generate Markov process and present the results of $L = 16$ with typical sweep number for single run as $50000 + 10 \times 5000$. Errors are estimated as standard deviation of 10 samples taken in the last half of each run. To locate the phase transition point, we calculate the internal energy U and the specific heat C defined as the thermodynamic averages as

$$\langle O \rangle \equiv \frac{1}{Z} \int [dU][dz] O[U, z] e^{A[U, z]}, \quad U = \frac{1}{L^4} \langle -A \rangle, \quad C = \frac{1}{L^4} \langle (A - \langle A \rangle)^2 \rangle, \quad (6)$$

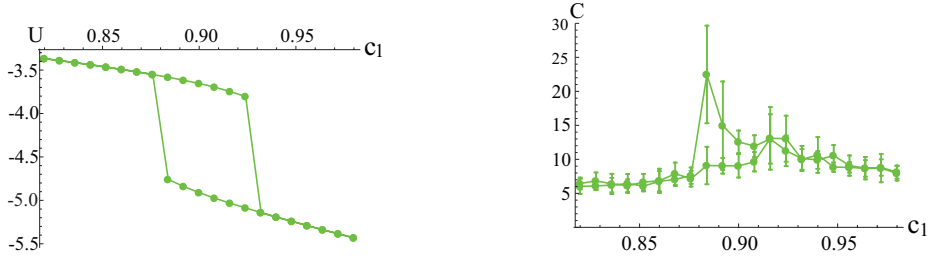


Fig. 1. $U(c_1)$ (left) and $C(c_1)$ (right) for $c_2 = 0.9$. U shows a hysteresis between $c_1 \simeq 0.88 \sim 0.93$. C shows double peaks near the edges of hysteresis.

where Z and A are given in Eqs. (2), (3). We measure U and C as a function of c_1 for a fixed value of c_2 (and vice versa). Location of phase transition point is determined from their behavior as follows;

(i) If $U(c_1)$ shows hysteresis while c_1 makes a round trip, it exhibits a first-order transition. Such hysteresis effect should diminish as MC runs more sweeps and leaves a gap $\Delta U(c_1)$ at the transition point $c_1 = c_{1c}$ ($\Delta U(c_1) \equiv \lim_{\epsilon \rightarrow 0^+} [U(c_1 + \epsilon) - U(c_1 - \epsilon)]$).

(ii) If $U(c_1)$ shows no hysteresis, but $C(c_1)$ has a peak developing as L increases and/or a gap of $\Delta C(c_1)$ appears at $c_1 = c_{1c}$, a second-order transition takes place there.

As typical examples of these transitions, we show the following three figures; In Fig. 1 we show U and C for $c_2 = 0.9$. U exhibits a hysteresis curve around $c_1 \sim 0.9$ and a first-order transition takes place. In Fig. 2 we show U and C for $c_2 = 0.4$. C exhibits a peak around $c_1 \simeq 1.63$ at which a second-order transition takes place. In Fig. 3 we show U and C for $c_2 = 2.0$. C exhibits a small jump which we take as a sign of a gap ΔC implying a second-order transition.

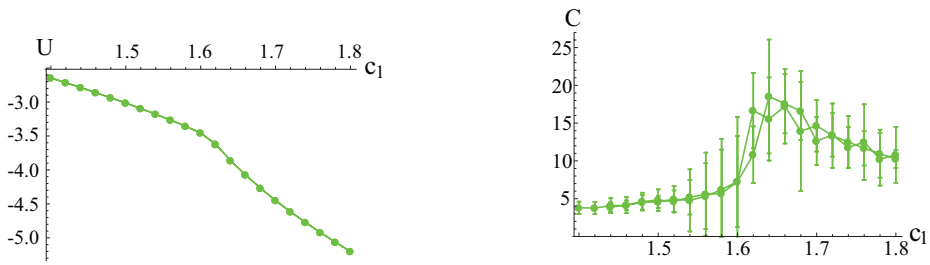


Fig. 2. $U(c_1)$ (left) and $C(c_1)$ (right) for $c_2 = 0.4$. $C(c_1)$ shows a peak at $c_1 \simeq 1.64$, at which a second-order transition takes place.

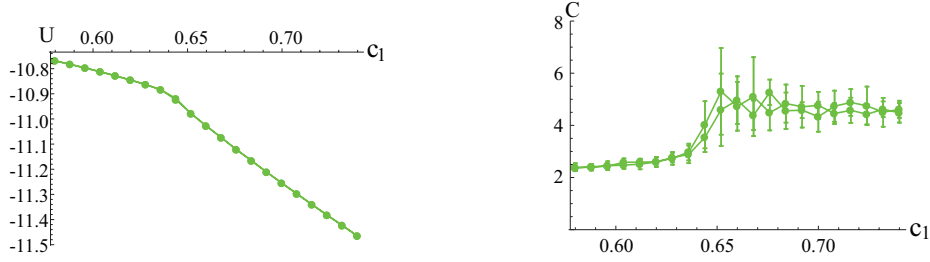


Fig. 3. $U(c_1)$ (left) and $C(c_1)$ (right) for $c_2 = 2.0$. $C(c_1)$ has a jump at $c_1 \simeq 0.65$ which we judge as a gap $\Delta C \neq 0$, implying a second-order transition.

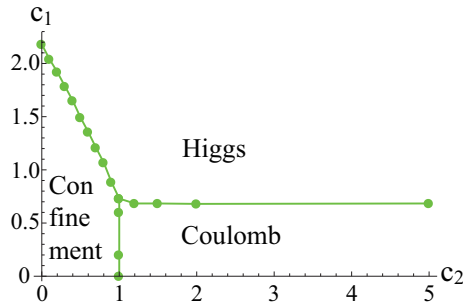


Fig. 4. Phase diagram of the 4D $CP^1+U(1)$ model (2) in the c_2 - c_1 plane determined by the MCS for the lattice $L = 16$. The transition between Coulomb and Higgs phases is of second-order. The confinement-Coulomb transition is of weak first order (almost second order), The confinement-Higgs transition is (i) first-order near the triple point, i.e., for $0.6 \lesssim c_2 \lesssim 1.0$, and (ii) second-order for $c_2 \lesssim 0.6$.

In Fig. 4 we show the phase diagram in the c_2 - c_1 plane. There are three phases as indicated. To identify each phase as shown there we measured squared electric field W_E , squared magnetic field W_B , and the magnetic monopole density Q [11] defined as follows;

$$\begin{aligned}
 W_E &\equiv \frac{1}{3L^4} \sum_{x,i} \langle (E_{x,i} - \langle E_{x,i} \rangle)^2 \rangle = \frac{1}{3} \sum_{x,i} \left[c_2 \langle \cos \theta_{x,0i} \rangle - c_2^2 \langle \sin^2 \theta_{x,0i} \rangle \right], \\
 W_B &\equiv \frac{1}{3} \sum_{x,i < j} \langle \sin^2 \theta_{x,ij} \rangle, \\
 Q &\equiv -\frac{1}{2} \sum_{i,j,k} \epsilon_{ijk} \langle n_{x+i,j,k} - n_{x,jk} \rangle = \frac{1}{4\pi} \sum_{i,j,k} \epsilon_{ijk} \langle \tilde{\theta}_{x,jk} - \tilde{\theta}_{x,jk} \rangle, \quad (7)
 \end{aligned}$$

where i, j, k takes 1, 2, 3 and we decompose $\theta_{x,ij} = \nabla_i \theta_{xj} - \nabla_j \theta_{xi}$ as $\theta_{x,ij} = 2\pi n_{x,ij} + \tilde{\theta}_{x,ij}$, ($-\pi < \tilde{\theta}_{x,ij} < \pi$). $n_{x,ij} \in \mathbf{Z}$ describes nothing but the Dirac string (quantized magnetic flux). In short, W_E measures the magnitude of fluc-

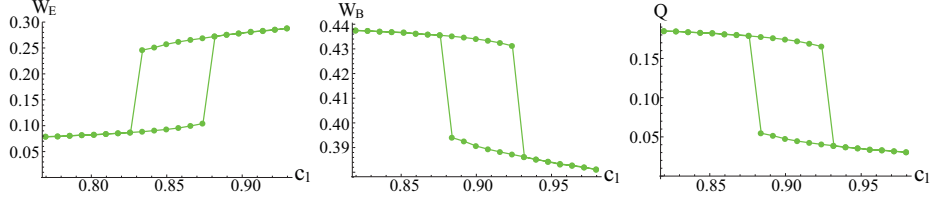


Fig. 5. $W_E(c_1)$ (left), $W_B(c_1)$ (middle), $Q(c_1)$ (right) for $c_2 = 0.9$.

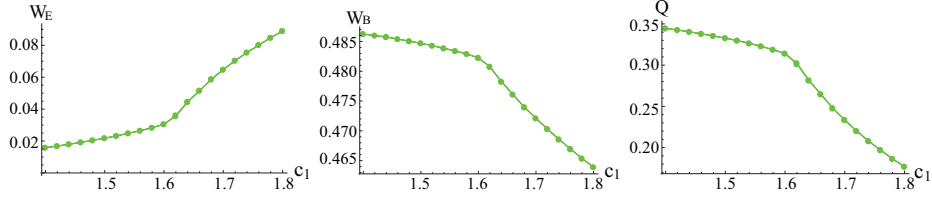


Fig. 6. $W_E(c_1)$ (left), $W_B(c_1)$ (middle), $Q(c_1)$ (right) for $c_2 = 0.4$.

tuations of electric field \mathbf{E} , and W_B and Q measure fluctuations of magnetic field $\mathbf{B} = \text{rot}\mathbf{A}$. Because vector potential \mathbf{A} and \mathbf{E} are canonically conjugate each other, uncertainty principle $\Delta\mathbf{A}\Delta\mathbf{E} \sim \Delta\mathbf{B}\Delta\mathbf{E} \gtrsim \text{const.}$ holds. In confinement phase, $\Delta\mathbf{E} \simeq 0$ and $\Delta\mathbf{B}$ is large. In the deconfinement phase such as Coulomb and Higgs phases, $\Delta\mathbf{E}$ is large and $\Delta\mathbf{B}$ is small. $\Delta\mathbf{B}$ is smaller in the Higgs phase than the Coulomb phase. We show these quantities for three values of c_2 shown in Figs. 1, 2, 3; $c_2 = 0.9$ in Fig. 5, $c_2 = 0.4$ in Fig. 6, $c_2 = 2.0$ in Fig. 7. In general, in the small- c_1 phase, W_B is large and W_E small, and in the large- c_1 phase, other way around. From these properties, it is straightforward to identify three phases as shown in Fig. 4.

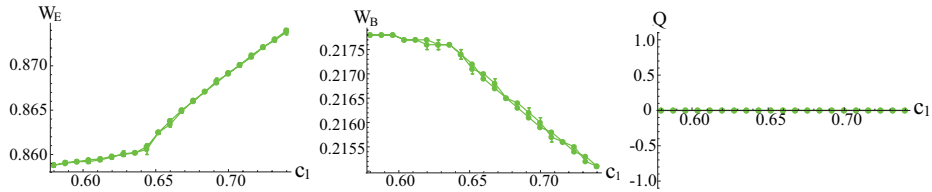


Fig. 7. $W_E(c_1)$ (left), $W_B(c_1)$ (middle), $Q(c_1)$ (right) for $c_2 = 2.0$. Q almost vanishes here due to strong suppression of monopoles due to large c_2 , while fluctuations in zero-monopole sector generate small but finite W_B .

3.2 Effect of Quantum and Thermal Fluctuations

To discuss the effect of quantum fluctuations, we introduce a classical model corresponding to the present quantum model (2). It is the 4D $Z(2)$ gauge theory defined by the action of Eq. (5) with the choice $S_x = \pm 1$ and $J_{x,x+\mu} = J_{x+\mu,x} = \pm 1$. These $Z(2)$ variables are discrete and express thermal fluctuations but no quantum fluctuations. In Fig. 8 we show the phase diagrams of these two models obtained by MCS. It shows that the region of Higgs phase is smaller in the $CP^1+U(1)$ model than in the $Z(2)$ model. Therefore we conclude that the quantum fluctuations in the present model generally reduce both abilities of learning patterns and recalling them (see Table I).

So far we considered the case of no noises ($T = 0$). In contrast with $T = 0$, the high-temperature limit $T \rightarrow \infty$ implies $N_0 \rightarrow 1$ in $\beta = N_0 a_0$; i.e., the $CP^1+U(1)$ model put on the 3D cubic lattice. Therefore, the effect of noises in signal propagations is estimated by comparing the results of the 4D model and 3D model with the same set of variables and action. In Fig. 9 we show the phase diagrams of the 3D model obtained by MCS[12] together with that of the 4D model in Fig. 4. In the 3D model, the confinement-Coulomb transition becomes a crossover and Coulomb phase disappears. Furthermore, the region of Higgs phase is smaller than that of the 4D model. Therefore we conclude that the thermal fluctuations in the present model generally reduce both abilities of learning patterns and recalling them.

4 Conclusion

We introduced the $CP^1+U(1)$ gauge theory on a 4D lattice as a microscopic model of quantum brain dynamics. It describes a system of molecules of bound water and photons in the brain and respects $U(1)$ gauge symmetry of the electro-

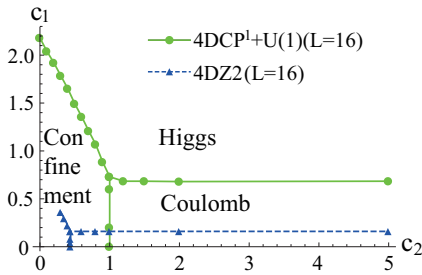


Fig. 8. Phase diagrams by MCS for 4D $Z(2)$ model and 4D $CP^1+U(1)$ model. Higgs region is smaller in the $CP^1+U(1)$ model. The transition line of the $Z(2)$ model terminates at $c_2 \simeq 0.28$.

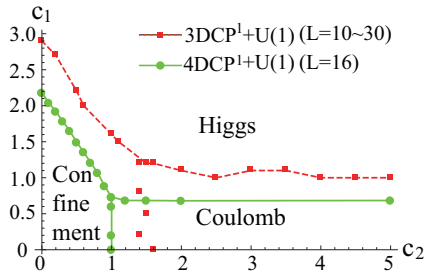


Fig. 9. Phase diagrams by MCS for 3D and 4D $CP^1+U(1)$ lattice gauge models. Higgs region is smaller in the 3D model. The 3D model has no Coulomb phase and the marks at $c_2 \simeq 1.4 \sim 1.6$ show the crossover.

magnetism. This model may be regarded also as a neural network of the brain after coarse graining. We calculated its phase diagram and compared it with related models. We found that both quantum fluctuations and thermal fluctuations by noise reduce the ability of learning and recalling patterns. We plan to confirm this point by an explicit simulation of learning processes.

Finally, we comment on the network structure of the $CP^1+U(1)$ model. To be realistic, the human brain has complicated network structures, such as left and right hemispheres, multilayer-structure, column-structure, small-world network, etc. Because the way to coarse-grain the microscopic model is not unique by itself, additional argument is required to explain the realistic brain structure. On this point, it is interesting to define the coarse-grained $CP^1+U(1)$ models on these networks and study their phase diagrams. Although we expect the basic three phases appeared in Table I, the details should be structure-dependent and shed some light on the study of brain architecture.

Acknowledgment

The authors thank Prof. K. Sakakibara and Dr. Y. Nakano for discussion. This work was supported by JSPS KAKENHI Grant No. 26400412.

References

1. J. J. Hopfield, Proc. Nat. Acad. Sci. USA. **79**, 2554 (1982).
2. D. O. Hebb, *The Organization of Behavior: A Neuropsychological Theory*, New York: Wiley (1949)
3. See, e.g., S. Haykin, "Neural Networks; A Comprehensive Foundation", Macmillan Pub. Co. (1994).
4. T. Matsui, in *Fluctuating Paths and Fields*, ed. by W. Janke et al., World Scientific (2001)271 (arXiv:cond-mat/0112463); M. Kemuriyama, T. Matsui and K. Sakakibara, Physica A **356**, 525 (2005) (arXiv:cond-mat/0203136); Y. Takafuji, Y. Nakano, and T. Matsui, Physica A **391**, 5258 (2012).
5. Y. Fujita, T. Hiramatsu, and T. Matsui, Proceedings of International Joint Conference on Neural Networks (Montreal, Canada, 2005) 1108. There is a similar model describing each neuron state by $U(1)$ variables instead of CP^1 variable; Y. Fujita and T. Matsui, Proceedings of 9th International Conference on Neural Information Processing, ed. by L.Wang et al. (2002)1360 (arxiv:cond-mat/0207023).
6. C. Stuart, Y. Takahashi and H. Umezawa, J. Theor. Biol. **71**, 605 (1978) ; Found. Phys. **9** (1979) 301; L. M. Ricciardi and H. Umezawa, Kybernetik **4**, 44 (1967).
7. M. Jibu and K. Yasue, Informatica **21**, 471 (1997); "Quantum Brain Dynamics. An Introduction", John Benjamins, Amsterdam (1995); See also G.Vitiello, Int. J. Mod. Phys. B **9**, 973 (1995) .
8. K. Wilson, Phys. Rev. D **10**, 2445 (1974).
9. H. J. Rothe, *Lattice Gauge Theories: An Introduction*, World Scientific (2005).
10. R.P.Feynman, "Statistical Mechanics, A set of Lectures", Chap.8, (W.A.Benjamin,1972).
11. T. A. DeGrand and D. Toussaint, Phys. Rev. D **22**, 2478 (1980).
12. S. Takashima, I. Ichinose and T. Matsui, Phys. Rev. B **72**, 075112 (2005).